https://doi.org/10.46813/2026-165-008

BGOOD COLLABORATION AND SEARCH FOR UNCONVENTIONAL BARYON STATES IN LIGHT *uds* QUARK SECTOR

V.B. Ganenko on behalf of BGOOD Collaboration
National Science Center "Kharkiv Institute of Physics and Technology", Kharkiv, Ukraine
E-mail: ganenko@kipt.kharkov.ua

It was reviewed the BGOOD photoproduction experiments at the ELSA electron accelerator at the University of Bonn (Germany) in the strange and non-strange baryon sectors. The BGOOD experiment was specifically designed to measure these processes at low momentum transfer to the residual hadron system, thus it was especially suited to search exotic molecular-like baryon states in light quark sector (*uds*) which could be equivalent to pentaquark P_C states observed in the *c*-sector. Results on the coherent photoproduction of the $\pi^0\pi^0$-, $\pi^0\eta$- and $\pi^0\pi^0\pi^0$-mesons on the deuteron demonstrate large differential cross sections, the mechanism of which is unclear: whether this is due to dibaryons or to rescattering processes.

PACS: 13.60.Le, 25.20.-x

INTRODUCTION

The BGOOD experimental facility [1] was located at the Electron Stretcher Accelerator (ELSA) at the University of Bonn (Germany) and was complemented to CBELSA/TAPS facility placed on the other ELSA beam line [2, 3]. Both facilities were aimed to study hadron spectroscopy in reactions of meson photoproduction in the resonance region (up to ~3.2 GeV), but BGOOD experiment was specifically designed to measure these processes at low momentum transfer to the residual hadron system, thus it was especially suited to search exotic and molecular-like baryon states.

Hadron spectroscopy is an important field of hadron physics aimed on studying fundamental problems about the nature of matter, e.g., such as the formation of the visible mass of the Universe from small mass quarks and massless gluons [4, 5]. Analyzing current development of the hadron physics, the Nuclear Physics European Collaboration Committee (NuPECC), which monitors the state of nuclear physics in Europe, notes in the report Long Range Plan 2024 for European Nuclear Physics [5]: "Hadron spectroscopy is subject to major experimental endeavors worldwide, poised to significantly change the nuclear physics landscape in the years ahead. Anticipated breakthroughs on the spectrum of ordinary and exotic hadrons are expected from CLAS12 and GlueX at JLab, BESIII, AMBER at CERN-SPS, ELSA, MAMI, the LHC experiments at CERN, Belle II, and in the long-term future, PANDA at FAIR as well as ePIC at EIC. These facilities utilize complementary probes and production mechanisms, crucial for understanding the symmetries governing the meson and baryon multiplets: photoproduction with polarized beams and target (MAMI, ELSA, GlueX), electroproduction (CLAS12); meson beams (AMBER, HADES, J-PARC); e+e-annihilation (BESIII, Belle II); ep (ePIC @ EIC), *pp* and heavy-ion collisions (LHC); and pp^-annihilations (PANDA), all of which are needed for studying different properties" (p. 19, 20).

Impressive research advances have been achieved thanks to the wide range of the facilities available to researchers, featuring diverse beams of hadrons, leptons, and photons, covering a vast energy range from nuclear physics to particle physics. Europe has played and continues to play a leading role in these researches. Therefore, based on the analysis conducted, NuPECC recommends [5]: (i) "Vigorous exploitation of the full physics potential offered by the recent upgrades of the electron facilities available in Europe at different energy scales (including ELSA, LNF, MAMI, S-DALINAC); (ii) Continuing support of the successful hadron physics programs in Europe and the participation of European groups at global facilities. Particularly important hadron physics facilities are: AMBER at CERN, Switzerland; ELSA in Bonn, HADES at GSI, MAMI and MESA in Mainz, Germany; Jlab in Newport News, USA" (p. 31).

There are two research directions in the hadron physics in the light and strange baryon range, which the NuPECC considers as priority, and which will be implemented in the coming years at the ELSA, MAMI, and JLab facilities. One of them includes identifying the "missing" states predicted by quark models (about two-thirds of which have not yet been observed experimentally) and searching for exotic hybrid baryon states. "Photoproduction measurements of the full set of polarization observables at MAMI and ELSA will further constrain partial wave analyses and lead to unique identification of excited nucleons" ([5], p. 20).

Another direction is the search for dibaryon states and determination of their properties. "Dibaryons provide another way to study baryon-baryon interactions, in particular by using dibaryons with a compact hexaquark structure. Hexaquarks are also of interest in the context of neutron stars, as they are bosons and therefore not subject to the Pauli exclusion principle during the formation of dense nuclear matter. The first hexaquark candidate to be experimentally detected is d*(2380), discovered by WASA at COSY. It is anticipated that the properties of the d*(2380) dibaryon, such as electric quadrupole moments, magnetic octupole moments, and transition form factors, will be studied through experimental programs at MAMI, ELSA, and JLAB" ([5], p. 25). These facilities also provide an ideal environment for training future generations of scientists and technical specialists.

The hadron spectroscopy program has been ongoing by the BGOOD collaboration for over 15 years, which is currently comprised of 18 scientists from Germany, Italy, Ukraine and USA (see the Appendix A for a full list). During this time, studying unconventional the multi-quark baryon states in the strange sector was the overarching motivation of the BGOOD photoproduction experiments. The results are presented in many papers and reports (see [6–8] and references therein).

At the end of 2025 experiments at the ELSA have been stopped for upgrade the facilities in accordance with new project called INSIGHT [6–8]. The project involves merging the BGOOD and CBELSA/TAPS photoproduction experiments at ELSA, upgrading the detectors, and expanding the capabilities of the facility for polarization measurements. And it is a part of broader research program in the field of fundamental physics that will be carried out by research teams from Bonn, Dortmund, Siegen and Jülich within a special Cluster of Excellence "Color meets Flavor" [9].

This article provides a brief overview of the BGOOD experimental setup and the results of the search for unconventional baryon and dibaryon states conducted by the BGOOD collaboration, as well as future research directions in this area.

1. THE STANDART MODEL OF PARTICLE PHYSICS

The Standard Model of Particle Physics (SM) [10] is physical theory which at present time explains a significant part fundamental subatomic processes in the Universe. It includes three of the four main interactions in nature, excluding gravity, classify all known elementary particles and underlies the modern scientific worldview. However, it is not a complete theory of fundamental interactions. It does not explain neutrino oscillations and their non-zero masses, why there is more matter than antimatter in the world, and leaves unexplained physical phenomena deduced from observational cosmology: the accelerated expansion of the Universe, and does not contain dark matter particles. Therefore, the SM can be considered as a basis for constructing more complete and accurate models.

It is based on discovered elementary particles, Fig. 1.1 – twelve fermions and four vector gauge bosons, performing interactions between the fermions. The fermions have spin ½ and are separated into two groups of six particles each – leptons and quarks, arranged in three generations. Each fermion has his antiparticle. Currently, elementary particles are considered as point objects that have no internal structure.

Quarks are divided into two groups: light *uds* (up, down, strange) quarks with masses $m_u \approx 2.2$ MeV, $m_d \approx 4.7$ MeV, $m_s \approx 95$ MeV, and heavy *cbt* (charm, bottom, top) quarks with masses $m_c \approx 1.28$ GeV, $m_b \approx 4.18$ GeV, $m_t \approx 173.1$ GeV. The interaction between them occurs through the exchange of vector gauge bosons with spin 1 – gluons, photons, as well as $W^{\pm}$ and Z bosons in the case of strong, electromagnetic and weak interactions, respectively. Higgs boson is responsible for generating masses of the fermions, $W^{\pm}$ and Z bosons.

The theory describing strong interaction of quarks is Quantum Chromodynamics (QCD). According to the QCD each quark has one of three possible color charges – red (r), green (g), and blue (b). Their antiparticles have a corresponding anti-color charge. The gluons can have eight independent color states, which are combinations of color and anti-color. This property of the gluons allows them to interact with each other that leads to major qualities of the QCD. One of them is effect known as asymptotic freedom. It is resulted from energy dependence of the strong coupling constant $\alpha_S(Q^2)$, which determines strength of the interaction of a gluon with other ones or a quark. The coupling constant decreases with the quarks energy increasing so that they behave like quasi-free particles at high energy, and perturbative QCD can be applied to describe the interaction processes in this case.

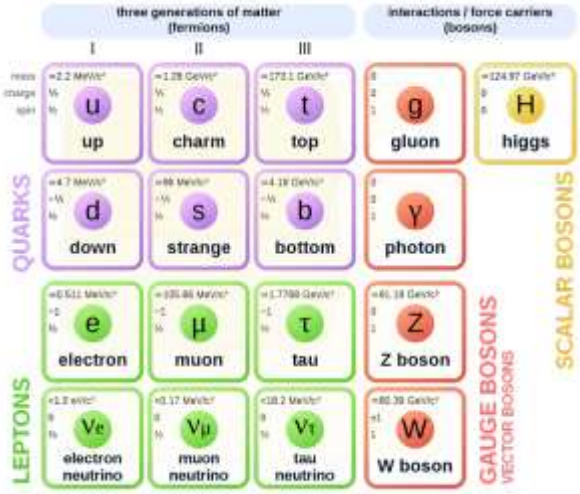


Fig. 1.1. Particles of the SM. Figure from Ref. [11]

The opposite effect is observed at low energies, when the constant $\alpha_S(Q^2)$ becomes large, leading to a very strong interaction between quarks and gluons, as well as between the gluons themselves. As a result, in addition to the constituent quarks, a multitude of virtual quarks and gluons (a "cloud" or "sea") are formed in the hadron. Therefore, the contribution of the constituent quarks to the hadron mass is small; for example, for the proton, it is about ~1%. The remaining mass (~99% of the hadron mass) is created by the energy of the internal gluon color field, which creates a "cloud" ("sea") of virtual quarks and gluons bound in the hadron. Thus, the strong interaction between quarks and gluons at low energies, firstly, leads to a fundamental effect, such as the generation of dynamical mass, which accounts for ~99% of the mass of observable matter in the Universe.

Secondly, this phenomenon produces the color confinement effect, which posits that isolated free quarks and gluons cannot appear and the observed objects are always confined to color singlet states. In order to produce such state, the quarks have to be bound in systems of several quarks. The conventional hadrons are realized most simply in either quark-antiquark ($q\bar{q}$) pairs (mesons) or three quarks (qqq) systems (baryons). The mesons and baryons are grouped into multiplets. The ground-state multiplets in the light quark sector are presented in Figs. 1.2a; 1.2b.

However, QCD does not exclude the existence of so-called unconventional, exotic objects consisting of more quarks than ordinary hadrons, and also bound gluon states. In the baryon sector, these can be pentaquark systems ($qqqq\bar{q}$), and in the meson sector, tetraquarks consisting of two quark-antiquark pairs ($q\bar{q}q\bar{q}$).

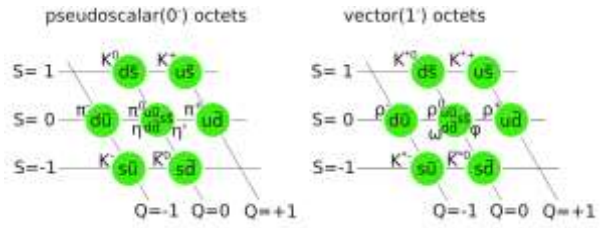


Fig. 1.2a. Octet plus singlet of the pseudoscalar ($J^P=0^-$) and vector ($J^P=1^-$) meson.

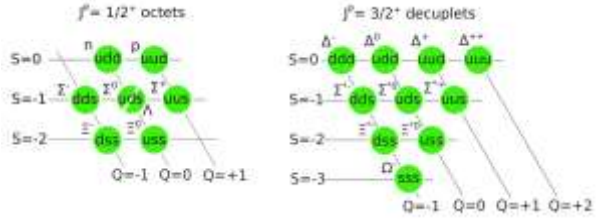


Fig. 1.2b. Octet plus decuplet of the ground state baryons. S shows strangeness and Q the charge of the particle. Figures from Ref.[12]

Furthermore, due to gluon self-binding, formations consisting solely of bound gluons, glueballs (*gg*,*ggg*) or of quark-antiquark pair and an excited gluon, hybrids ($q\bar{q}g$*), may also exist. Such quark systems can exist not only as compact quark-gluon objects, but also in a molecular state consisting of either nucleon and meson or two mesons, as shown in Fig. 1.3.

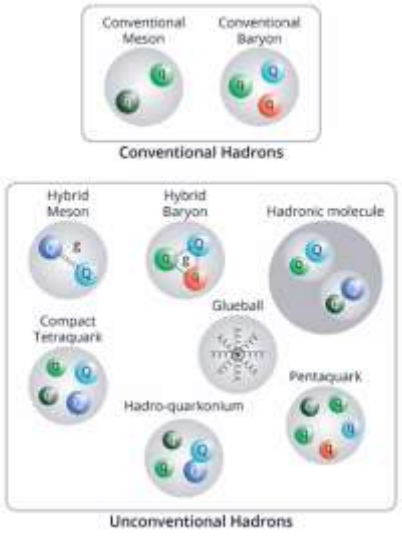


Fig. 1.3. Valence content of conventional and unconventional (exotic) hadrons. Figure from Ref. [5]

During the past twenty years a large number of exotic states (pentaquarks and tetraquarks) have been discovered in the heavy quark sector. The first tetraquark state $X(3872)$ was discovered in 2002, and currently these states form the large group of XYZ mesons [13]. The pentaquark states P_C with quark content ($uudc\bar{c}$) were discovered at LHCb in 2015, but the data with higher statistical precision and mass resolution were obtained in 2019 [14]. The internal structure of these states is still unclear, but as many reside close to meson–baryon or meson–meson production thresholds, there are strong arguments that they are extended molecular-like systems of hadrons bound via pion exchange and being analogs of light nuclei [13]. Besides, there is growing evidence that similar structures may be seen in the (*uds*) sector [6, 15].

The large amount of experimental data that has not yet been explained has led to an intensification of research in the field of hadron spectroscopy and the search for unconventional exotic states. In addition to the BGOOD collaboration, other GeV-range facilities are also participating in these studies: CLAS and GlueX at Jefferson Lab [16], A2 at MAMI [17], Crystal Barrel at ELSA [2, 3], LEPS at SPring8 [18], GRAAL at ESRF [19]. Access to low momentum exchange is mandatory to elucidate the role of molecular-like structure if they are loosely bound and spatially extended systems. In photoproduction experiments with a fixed target this corresponds to forward meson acceptance to ensure the recoiling hadron system has minimal momentum transfer. The BGOOD facility is specifically designed to study hadronic spectroscopy at low momentum transfer to the residual hadron system.

2. THE BGOOD EXPERIMENTAL FACILITY

The BGOOD experimental facility was located at one of beam lines of the Electron Stretcher Accelerator (ELSA) at the University of Bonn, Germany. The facility included: (i) a system of photon beam tagging and intensity control; (ii) a central detector consisting of an electromagnetic calorimeter for identifying neutral mesons via detection of decay photons and determination their four-momenta; cylindrical scintillator barrel and multi-wire proportional chambers for charge particles selection; (iii) a forward spectrometer for charged particle identification at forward angles and their momentum reconstruction; (iv) cryogenic hydrogen or deuterium targets. The BGOOD facility was described in details in many publications, e.g. [1], so it will provide a brief description here.

2.1. THE ELSA ACCELERATOR FACILITY

The ELSA accelerator facility is shown in Fig. 2.1. There are two electron sources, which are produced either polarized or unpolarized electrons. The electrons were injected into a LINAC and accelerated up to an energy of 26 MeV. Then the electron beam was transferred to the booster synchrotron of 69.9 m circumference. The booster runs with a fixed cycle time of 20 ms, accelerating electron beams usually up to 1.2 GeV (maximal energy is 1.6 GeV). When needed energy was reached, the beam was extracted and transferred to the stretcher ring with a circumference of 164.4 m. Several injections from the booster synchrotron were accumulated in the stretcher ring that a homogeneous filling of the ring was obtained. When the stored current reached a 20…25 mA the injection process was stopped and the stored electron beam was accelerated up to the needed energy (maximum energy

is ~3.2 GeV) and then was slowly extracted to facilities BGOOD [1] or Crystal Barrel [2, 3]. Typical extracted current for the experiment was ~0.5…1.2 nA, the extraction duration was 4…15 s, giving a duty factor of 70…90%. The extracted beam had a micro-structure of electron bunches separated by 2 ns.

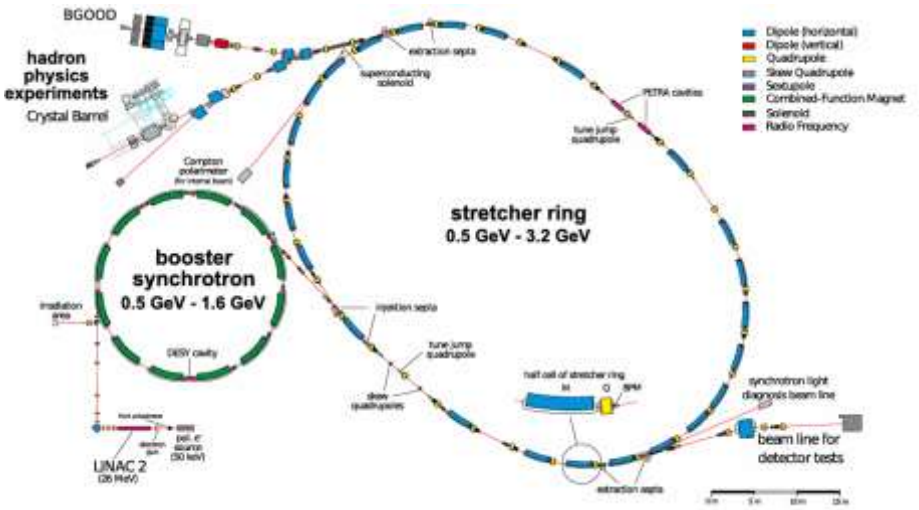


Fig. 2.1. Overview of the ELSA accelerator facility. Figure from Ref. [1]

2.2. THE PHOTON TAGGER AND BEAM INTENSITY CONTROL

The Photon Tagger was used to determine energy and time of the produced photon. Its scheme is shown in Fig. 2.2. The primary electron beam was directed onto photon radiator (0.56 mm thick diamond crystal or copper foil) fixed in a goniometer. It had a Gaussian distribution with a full width at half maximum (FWHM) of 2.9 and 0.7 mm in the horizontal and vertical directions respectively. Photon energy, E_γ, was defined as the difference between the energy of the initial electrons, E_0, and their energy after photon emission, E.

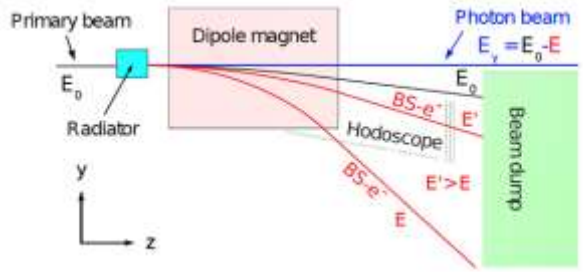


Fig. 2.2. Scheme of the Photon Tagger. An electron beam with energy E_0 is incident on a photon radiator. Some of the electrons lose energy as a result of bremsstrahlung and emit photons with energy $E_\gamma = E_0 - E$. BS–e^- is the electron trajectory after bremsstrahlung. Figure from Ref. [1]

The energy of the latter was determined by deflecting these electrons in the magnetic field of a dipole magnet, which was measured using a scintillation hodoscope. It consisted of 120 plastic scintillators, and was split into two parts: the horizontal part provided measurements of the post-bremsstrahlung electrons in energy range (0.1…0.3)E_0 with resolution of ~0.4%E_0. The vertical part covered the energy range (0.3…0.9)E_0 and has resolution (0.6…1.7%)E_0. For improving the resolution in the range (0.3…0.66)E_0, an additional detector ARGUS was used. It improved the resolution to (0.08…0.45%)E_0. A time resolution of the photon tagging was 200 ps.

The photon beam passed two lead collimators with hole diameters of 7 and 12 mm, and directed onto target located at the centre of BGOOD detector. The photon flux was controlled by a Flux Monitor (FluMo) which was situated at the end of the beam line. The FluMo consisted of five plastic scintillators placed in the beam line for measuring the relative flux of the photons using process of e^-e^+ pairs production. The FluMo detection efficiency was determined with a fully absorbing lead glass detector – the Gamma Intensity Monitor (GIM). The photon beam position was controlled by a photon camera. For details see [1].

2.3. THE BGOOD DETECTOR

2.3.1. Central detector

The BGOOD detector is shown in Fig. 2.3. It included a central detector and a Forward Spectrometer (FS). The central detector is shown in Fig. 2.4 in more details. It consisted of an electromagnetic calorimeter (BGO Rugby Ball) for gamma-quanta detection, a segmented Scintillator Barrel (SB) for charged particle identification, and two coaxial cylindrical multi-wire proportional chambers (MWPCs) for charged particle tracking and reaction vertex reconstruction.

BGO Rugby Ball. It was the main detector of the facility, shown in Fig. 2.4, consisting of 480 BGO crystals with a length of 24 cm (~21X_0). The crystals were arranged in 15 sectors of 32 crystals each. Each sector covered a full azimuthal ring, with the azimuthal angle capture $\Delta\varphi = 11.25^0$ and the polar angle capture $\Delta\theta = 6…10^0$ per crystal, respectively. The total angular capture of polar angles was $\theta = 25…155^0$. The energy resolution for 1 GeV photons was ~3% (FWHM). A time resolution was 2 ns.

For initial energy calibration, radioactive sources ^{22}Na with emitted photons energy of 1.27 MeV were used. They were placed inside the BGO Rugby Ball.

Then the calibration was proceeded by fitting to the π^0 mass from the observed $\pi^0 \rightarrow 2\gamma$ decay.

Neutral mesons identification is shown in Fig. 2.4. The BGO Rugby Ball detected also charged pions, protons and deuterons. Its total signal was used for trigger purposes. More details on the BGO Rugby Ball can be found in Ref. [1].

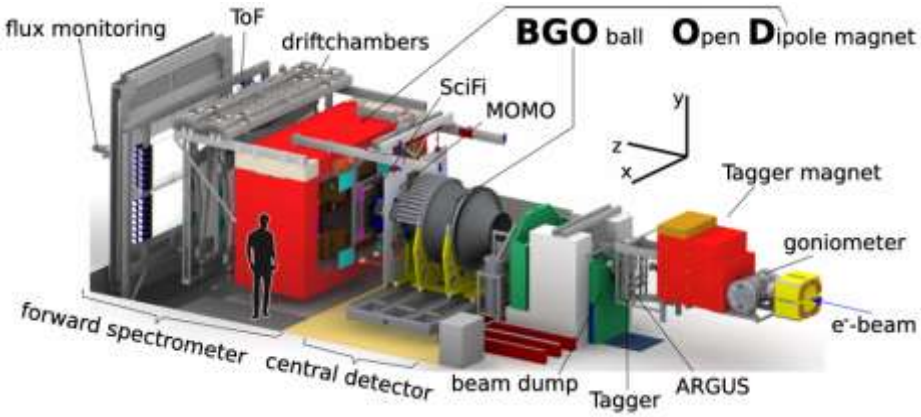


Fig. 2.3. Overview of the BGOOD setup. Figure from Ref. [1]

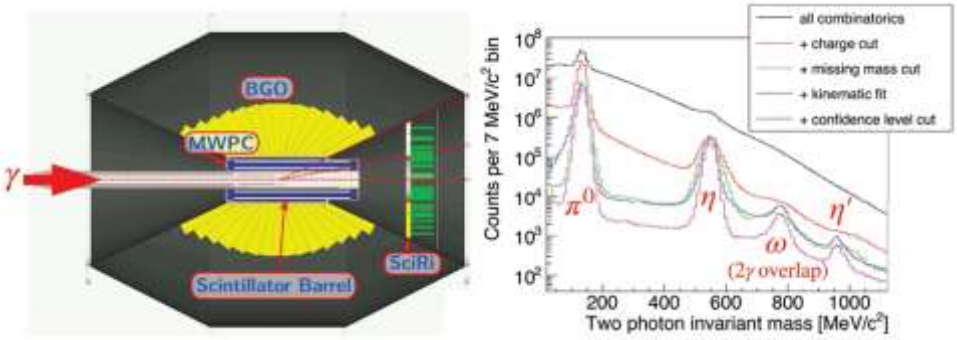


Fig. 2.4. Left: View of the central detector. Right: Neutral meson identification by the Rugby Ball. The selection cuts: there is no coincidence with the Scintillator Barrel, identifies the particles as neutral (red line); the mass recoiling from the two-photon system to be consistent with the proton mass (green); three-momentum conservation for the two photons and proton (blue); cut on the confidence level of 90% (magenta). Figures from Ref. [6]

Cylindrical MWPCs. Two MWPCs were used for charged particle tracking inside the BGO Rugby Ball. Inner and outer radiuses of the first were 48.2 and 56.2 mm, and the second one of 79.5 and 87.5 mm respectively, the length of both was 520 mm that result in a polar angular coverage of θ=8…163). Information obtained from the MWPCs allows the particle trajectory to be reconstructed with a resolution of $\delta z \approx 0.5$ mm along the beam axis, $\delta\varphi \approx 1.5^0$ in azimuth and $\delta\theta \approx 1^0$ in polar angle.

Scintillator Barrel. The Scintillator Barrel (SB) was placed between the BGO Rugby Ball and MWPCs and together with MWPCs was used to distinguish between neutral and charged particles. It consisted of 32 plastic scintillating bars 5 mm thick arranged in a cylinder with a radius of 9.8 cm. Charged particle identification was via $\Delta E{-}E$ techniques by comparing energy deposition in the SB and the BGO Rugby Ball and was ~98%.

Scintillator ring detector. The Scintillating Ring (SciRi) segmented detector was mounted inside the forward opening cone of the BGO Rugby Ball, as shown in Fig. 2.4. It covered the acceptance gap between the open forward cone of the BGO Rugby Ball and the rectangular gap of the Open Dipole magnet and was used for the charged particles direction reconstruction in the polar angular range $\theta=10\ldots25^0$, which were not detected by the BGO Rugby Ball. The individual plastic elements of 20 mm thick are arranged in three rings. Each ring consists of 32 segments, providing polar and azimuthal angle resolution of $\Delta\theta=5^0$ and $\Delta\varphi=11.5^0$. The time resolution of charged particle detection was ~3 ns.

2.3.2. Forward Spectrometer

The Forward Spectrometer (FS) was built around large Open Dipole magnet (OD), Fig. 2.5, and was used to select and identify charged particles at polar angles from 0.5 to 12^0. Charged particles were tracked in front of and behind the magnet. The final component of the FS was a time-of-flight (ToF) detector, located 5.6 m from the target.

Open Dipole magnet. The central element of the FS was an OD magnet, which allowed the momentum of charged particles to be measured and their charge sign determined. The magnet's gap dimensions were 54 cm (height)×84 cm (width)×150 cm (length). The magnetic field map was measured to determine particle trajectories within the magnet and the influence of edge magnetic field on their trajectories.

Front and rear tracking. Front charged particles tracking was performed by scintillating fibers detectors

MOMO and SciFi (Fig. 2.5). The MOMO had a diameter of 44 cm, with a central 4.5 cm hole to allow the photon beam to pass. It consisted of 672 fibers, each 2.5 mm in diameter. The fibers were arranged in three layers so that there was a 60^0 angle between the fibers of adjacent layers. The charged particle positions were determined by coincidence hits between either two or three fibers of the different layers. MOMO had a particle position reconstruction efficiency of 80%.

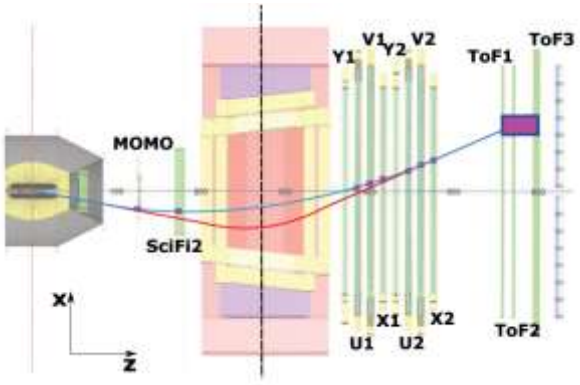


Fig. 2.5. The trajectory of a charged particle in the FS. The purple boxes indicate the hit positions in the various detectors. An initial tracking algorithm assumes a straight trajectory outside of the OD magnet, and a circular trajectory within (red line). This is later corrected to account for the non-uniform and extension of the magnetic field (blue line). Figure from Ref. [6]

The SciFi detector consisted of 640 fibers with a diameter of 3 mm. The fibers were arranged to form two 320 fibers layers, at an angle of 90^0 to each other, covering an active region of 66 cm in width and 51 cm in height. A 4×4 cm hole in the centre allowed the photon beam to pass. The combination of signals of both fiber layers determined the particle position with efficiency of 97.5%.

Tracking of charged particles behind the OD magnet was achieved using eight double-layer drift chambers with a sensitive area of 246×123 cm. For unambiguous track reconstruction, the wires were oriented in four different directions in the plane perpendicular to the beam axis: in the X and Y directions, and under $\pm 9^0$ to the *X*-axis. The drift chambers did not have a central hole, thus to avoid damage by the photon beam, central spots of 5×5 cm have been made insensitive.

Time-of-Flight detector. The ToF detector consisted of 3 walls an area of 3×3 m, made from 36 horizontally oriented plastic scintillator's bars. Each wall had a gap in the centre for the photon beam to pass. The readout was performed from each end of the bars with photomultiplier tubes. The position of the incident particle in the X direction along the bar was determined by the time difference of the two readouts, giving a resolution of ~20 cm. A time resolution was of 0.34 ns.

Trajectory reconstruction was achieved via description of particle motion between detectors and in the field of dipole magnet, taking into account their energy losses, and is shown in Fig. 2.5. The length of the trajectory was used to determine the particle speed β from the time measurements at the ToF walls. Fig. 2.6 shows the reconstructed particle β versus momentum and reconstructed mass, with characteristic loci of π^+, K^+ and protons. A momentum resolution of 3 to 6% was achieved when the OD magnetic field is operated at maximum or at half the maximum value respectively. For protons and deuterons, the momentum resolution can be improved to 3% if the β measurement was used instead of momentum and fixing the particle mass.

2.3.3. Cryogenic target system

The BGOOD experiment can use either solid or liquid cryogenic (hydrogen or deuterium) targets positioned at the center of the BGO Rugby Ball. The cryogenic target cell consisted of an aluminium hollow cylinder of 4 cm diameter, 0.5 mm wall thicknesses and 6 or 11 cm length. Beam entrance and exit windows were made of 0.1 mm thin Mylar foil.

For hydrogen target of 6 cm length this yields an area density of $0.425\ \mathrm{g\cdot cm^{-2}}$, corresponding to $2.53\cdot 10^{-7}\ \mu\mathrm{b}^{-1}$.

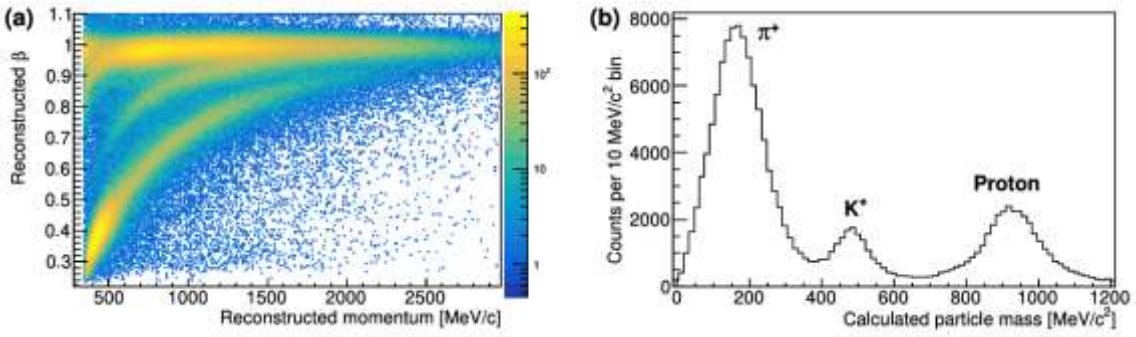


Fig. 2.6. Positively charged particle identification in the forward spectrometer. To accentuate the contribution from K^+, a π^0 was required to be identified in the BGO Rugby Ball, a photon beam energy over 900 MeV and a total energy deposition in the BGO Rugby Ball smaller than 250 MeV. Particle β versus momentum. Loci corresponding to π^+, K^+ and protons are evident (a). Calculated particle masses for particles with momentum between 600 and 1000 MeV/c (b). Figures from Ref. [6]

2.4. DATA TAKING

The data taking were made during 2017–2025 years, with usually two to three data taking about four week's periods per year. An electron beam with an energy of 2.9 GeV and current of 1.2 nA were typically used. The global triggers including local triggers for sub-detector components, and the corresponding triggering rates are

presented in the Table 1. The triggers were used to ensure that all reactions of interest were saved for further analysis. One million triggered events were saved approximately every 12 min, corresponding to a rate of 1.4 kHz. Thus very large massive of the data was obtained on strange meson photoproduction in the second resonance range.

The BGOOD simulation was based upon Geant4 [20] and accurately described the detector geometry, magnetic fields, and the energy and time resolutions which were measured from real data. Detector and trigger efficiencies were determined for every data taking period.

Table 1

Global trigger conditions. Low and high thresholds correspond to low and high energy sum depositions (typically 100 and 200 MeV). Table adapted from Ref. [6]

Trigger		
0	Tagger & BGO Rugby Ball (high thresh.)	750 Hz
1	Tagger & SciFi & BGO Rugby Ball (low thresh.)	400 Hz
3	Tagger & SciRi & SciFi & ToF	250 Hz
4	Tagger & SciFi & TOF & BGO Rugby Ball (low thresh.)	150 Hz

3. SEARCH FOR UNCONVENTIONAL BARYON STATES IN THE LIGHT QUARK SECTOR

Over the past twenty years quite a lot of exotic multiquark states have been reliably observed in the heavy quark sector, going beyond the valence quark-antiquark and three-quark systems. The pentaquark states with content ($uudc\bar{c}$), obtained from dataset with significantly increased statistics were presented by the LHCb collaboration in 2019 [14] – $P_c(4312)$, $P_c(4440)$ and $P_c(4457)$ (Fig. 3.1).

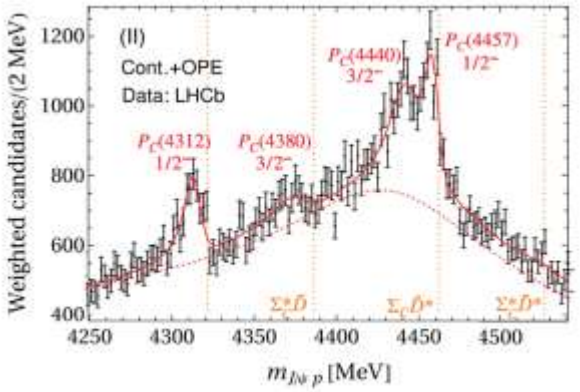


Fig. 3.1. The coupled channel analysis of Du et al. [21] fitted to the J/ψp invariant mass spectrum from LHCb [14]. The dotted curve represents the background. Labelled inset are the P_c states and their corresponding J^P when calculated as hadronic molecules. The $\Sigma_c^{(*)}\bar{D}^{(*)}$ thresholds are shown by vertical dotted lines. The $P_c(4380)$ is suggested by [21]. Figure from Ref. [6]

Because their masses were approximately 5, 20, and 2 MeV below thresholds the $\Sigma_c^*\bar{D}^*$ states respectively, the authors noted that this fact makes observed P_c good candidates for the bound states of these systems. This assumption was well consistent with description of the experimental data by coupled channel model of Du et al. [21], where the observed P_c states were considered as hadronic molecular states $\Sigma_c^*\bar{D}^*$ with corresponding J^P (see Fig. 3.1). The model predicted seven hadronic molecular states, three of which corresponded to the aforementioned pentaquarks. Another predicted state $\Sigma_c^*\bar{D}$ with $J^P=3/2^-$ and mass 4380 MeV/c^2, consistent with the experiment, was also proposed. It has mass ~15…20 MeV/c^2 below the $\Sigma_c^*\bar{D}$ threshold, thus it was identified as the pentaquark $P_c(4380)$.

Since all these states are narrow and below the $\Sigma_c^+\bar{D}^0$ and $\Sigma_c^+\bar{D}^{*0}$ thresholds within reasonable binding energies, they provide the strong experimental evidence to date for the existence of bound states of a baryon and a meson ($[duc][u\bar{c}]$) in charm sector.

If the strong interaction is flavor independent, similar molecular states can also exist in the light quark sector. In this case, the proposed analogue in *uds* sector should have a quark content obtained by replacing *c*-quarks with *s*-quarks as shown in Fig. 3.2, and should therefore lie near the $\Sigma^{(*)}K^{(*)}$ states thresholds.



Fig. 3.2. Parallels between charmed and strange sectors. Figure from Ref. [22]

The possible existence of hidden strange molecular pentaquarks consisting of the ΣK, ΣK*, and Σ*K* states was considered within the quark delocalization color screening model (QDCSM) [15]. In particular, it was suggested that the ΣK molecular pentaquark with quantum numbers $IJ^P=1/2^3/2^-$ could be considered a strange partner of the $P_C(4380)$ state.

Due to smaller masses, molecular structures incorporating *uds* quarks should be expected to have a priori larger width compared to the charmed sector. So they can manifest themselves in differential cross sections not as clearly defined narrow peaks, but as broader peaks or "cusps" and at low momentum transfer to the molecular hadronic system. The large amount of data obtained in the BGOOD experiment on the strange meson photoproduction has allowed to search parallels between the molecular structure in the charmed and strange sectors. A detailed analysis of the BGOOD results has been carried out in [6]. Table 2 presents three molecular-like states which could be considered as analogous to the observed P_c pentaquark states.

At present, the most reliable analogue was found between the $P_c(4382)$ and the $K^+\Sigma^0(1385)$ systems. Based on the *c* and *s* quarks exchange criterion, such molecular-like system should be observed as "a cusp-

like" structure in the differential cross section of $\gamma p \to K^+\Sigma^0$ reaction at W~1900 MeV, below the pK^+K^- threshold. From existing experimental data [28–32] only the BGOOD results [23] obtained at the angles $\cos\theta^K_{CM}>0.9$ demonstrate apparent presence of such "cusp-like" structure, Fig. 3.3. As was shown in [23], the cusp becomes visible when $\cos\theta_K{}^{CM} \geq 0.95$.

In order to make it more pronounced, the cross-section values were extrapolated to the angle $\cos\theta_K{}^{CM}=1$, Fig. 3.4. The fit of the extrapolated data by a sum of a fourth-order polynomial and a Breit-Wigner functions well describes the cross section and agrees with hypothesis on observation the $K^+\Sigma^0(1385)$ molecular system which is the strange analogue of the $P_c(4382)$.

Table 2 (from Ref. [6])

Comparison between P_C states, their proximity to $K\Sigma$ thresholds and evidence of molecular states in light quark uds sector

Charm sector		Strange sector	
Threshold	State	Threshold	Evidence
$\Sigma_c^- D$	Pc(4312)	$\Sigma^0 K^+$ at 1687 MeV	N(1535)
$\Sigma^*_c{}^- D$	Pc(4382)	$\Sigma^0(1385)K^+$ at 1879 MeV	Peak in $K^+\Sigma^0$ at t_{min} (BGOOD [23])
–	No equivalent	K^+K^-N at 1926 MeV	Structure in $K^+\Sigma^-$ at low t (BGOOD [24])
$\Sigma_c^- D^*$	Pc(4457)	$\Sigma^0 K^{*+}$ at 2085 MeV	Cusp in $K^0\Sigma^+$ (CB/ELSA-TAPS [25]) (Tentative) peak in $K^0\Sigma^0$ (BGOOD [26]) Triangle singularity in $K^+\Lambda(1405)$ (BGOOD [27])

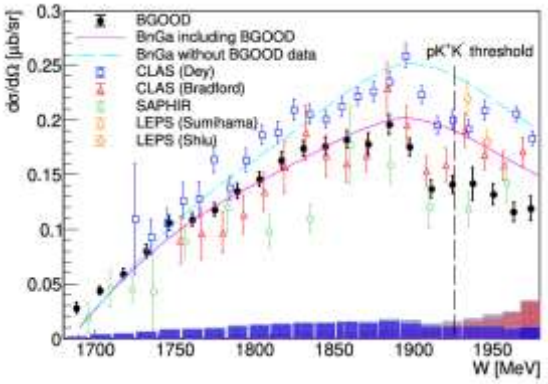


Fig. 3.3. $\gamma p \to K^+\Sigma^0$ differential cross section for angles $\cos\theta^K_{CM}>0.9$ (black circles). The systematic uncertainties on the abscissa are in three components described in Ref. [23]. Previous data [28–32] are additionally shown and labelled in the legend. The CLAS data are at the more backward angle of $0.85<\cos\theta^K_{CM}<0.95$. The Bonn–Gatchina PWA solutions [33] is shown with and without inclusion of the new data. Figure from Ref. [6]

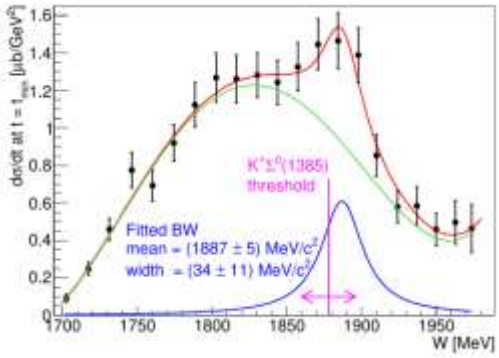


Fig. 3.4. $\gamma p \to K^+\Sigma^0$ differential cross section $d\sigma/dt$ extrapolated to t_{min} versus W. The sum of a fourth order polynomial and Breit-Wigner function is fitted to the data (red line, with constituent components in green and blue respectively). The fitted parameters of the Breit-Wigner and the $K^+\Sigma^0(1385)$ threshold are labelled inset. Figure from Ref. [6]

Similar molecular-like structure at $W\approx1920$ MeV with a width of ~50 MeV, close to the pK^+K^- threshold was observed in differential cross section on the $\gamma n \to K^+\Sigma^-$ reaction [24] (Fig. 3.5). But at present time it doesn't find any analog to it in the charmed sector. There are also indications on equivalence between the pentaquark $P_C(4457)$ and the $N^*(2030)$ states which are observed near the $\Sigma_c^- D^*$ and $\Sigma^0 K^{*+}$ thresholds respectively.

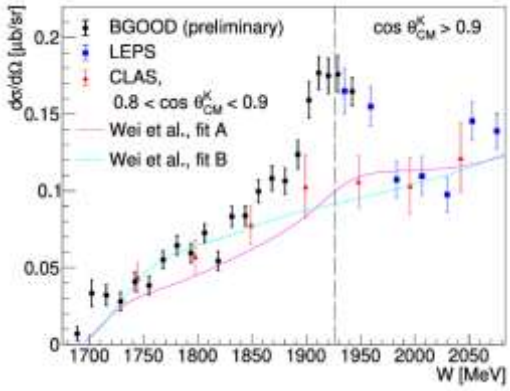


Fig. 3.5. Preliminary BGOOD data [24] on $\gamma n \to K^+\Sigma^-$ differential cross section and previous data from LEPS [34] and CLAS (at the angle of $0.8<\cos\theta^K_{CM}<0.9$) [35]. The model fits A and B of Wei et al. are described in Ref. [36]. The pK^+K^- threshold is indicated by the dashed line. Figure from Ref. [6]

The $\gamma p \to K^0\Sigma^+$ reaction cross section measured at CB/ELSA-TAPS [25] demonstrates a cusp stricture at $W\approx2100$ MeV, which is consistent with manifestation of the $N^*(2030)$ state and described by the coupled channel model [37]. According to calculations of this model, a similar peak arising from the $N^*(2030)$ state should also appear in the reaction $\gamma n \to K^0\Sigma^0$ (Fig. 3.6). Experimental data [26] is consistent with the calculation but higher statistical precision is required for any conclusive statement and support proposed equivalence between the $N^*(2030)$ resonance and the P_C states in the charm quark sector.

For the pentaquark $P_C(4312)$, which is assumed to be the $\Sigma_C\bar{D}$ molecular state, the equivalent molecular state in the light quark sector is believed to be the $N(1535)$ resonance, which is 150 MeV below the Σ^0K^+ threshold.

As a whole, the BGOOD experiment indicates the presence of significant evidence confirming the molecular-like structure of hadrons and the existence of analogues between the P_C and states in the *uds* quark sector. Many of them are close to a centre-of-mass energy of 1900 MeV and to multiple open and hidden strangeness thresholds, including K^+K^-p, ϕp, $f_0(980)p$, $a_0(980)p$, $K^+\Sigma(1385)$ and $K^+\Lambda(1405)$ systems [39]. The goal of the future experiment is to obtain a realistic picture and determine the main states that lead to the observed maxima in these reactions.

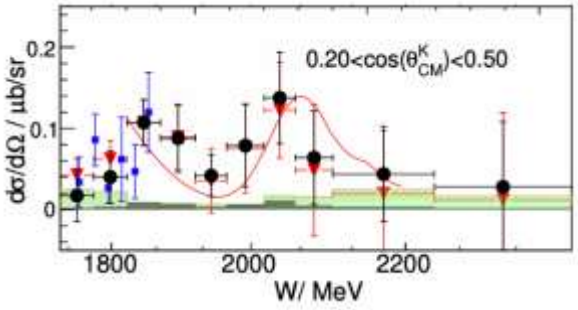


Fig. 3.6. $\gamma n \to K^0\Sigma^0$ differential cross section [26] for $0.2<cos\theta^K_{CM}<0.5$, employing two different fitting methods for yield extraction (red triangles and black circles). The blue squares are data from the A2 collaboration [38]. The predicted total cross section from Ref. [37] is shown as the red line at an arbitrary scale. Figure from Ref. [7]

4. COHERENT MESON PHOTOPRODUCTION OFF DEUTERON

Another direction of the BGOOD experiments is the search for dibaryon states, in particular, dibaryons with a compact hexaquark structure, and determination of their properties. The BGOOD collaboration has accumulated large amount of data on the cross sections of coherent pion photoproduction reactions $\gamma d \to \pi^0\pi^0 d$ [40], $\gamma d \to \pi^0\eta d$ [41], and $\gamma d \to \pi^0\pi^0\pi^0 d$ [42] (Fig. 4.1), which are promising for the dibaryons search.

The measurements were performed for deuteron emission angles $\cos\theta^d_{CM}>0.8$. These angles provide a momentum transfer to the deuteron that is an order of magnitude higher than the internal momentum of the nucleons in the deuteron (~80 MeV/c), so the cross section for a conventional coherent process is suppressed. In addition, the BGOOD setup provides a clearer separation of protons and deuterons, which allows eliminating the significant background associated with the quasi-free reaction of protons.

The most unusual aspects of the measurements are, firstly, the very large differential cross sections for these reactions, significantly exceeding those expected within the momentum approximation, and secondly, the similar shapes and values of these cross sections in certain energy ranges. This indicates that other mechanism predominate in this case, distinct from the reactions on free nucleon, where the reaction $\pi^0\eta N$ is significantly smaller than $\pi^0\pi^0 N$.

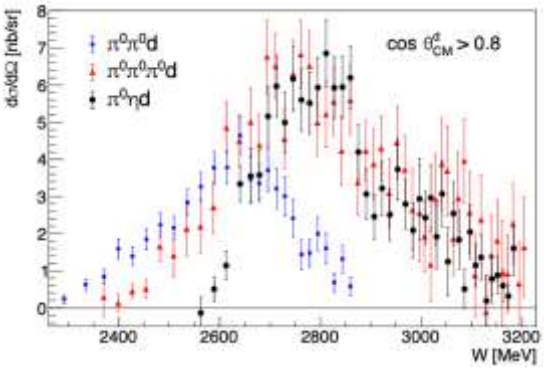


Fig. 4.1. Differential cross sections measured at BGOOD experiment for coherent photoproduction channels off the deuteron for $\cos\theta^d_{CM}>0.8$ [40–42]. The $\pi^0\pi^0\pi^0 d$ data are preliminary. Figure from Ref. [6]

4.1. DIBARYON STATES

Deuteron is the simplest nucleus composed of a bound proton and neutron with $IJ^p = 01^+$ (I-isospin, J-total angular momentum, p-parity) and can be considered as a typical molecular state, because its large spatial extent and mass, which is just below the pn disintegration threshold, are characteristic features of the hadronic molecules (dibaryons).

Dyson and Xuong model [43] predicts six non-strange dibaryon states D_{IJ}, shown in Fig. 4.2. They include the deuteron, D_{01}, the experimentally observed virtual state of two nucleons with mass 1.88 GeV/c^2, D_{10}, and four dibaryon states: D_{12} and D_{21}, which are the $N\Delta$ configurations with masses 2.16 and 2.17 GeV/c^2, and D_{03} and D_{30}, which are the $\Delta\Delta$ configurations with masses 2.35 and 2.47 GeV/c^2 respectively. To date, experiment have been indicated the existence of several candidates corresponding to the above dibaryon states.

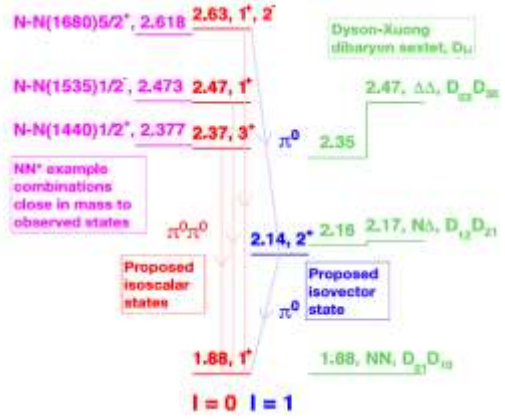


Fig. 4.2. The predicted Dyson-Xuong diboryon sextet is shown in green. The spectrum of dibaryon isoscalar (red) and isovector (blue) states with spin and parity proposed in [44], and possible configurations of bound $N\Delta^*$ states are shown in purple. Figure from [6]

First, it was isoscalar dibaryon $d^*(2380)$ with $IJ^P=03^+$, which was discovered by WASA collaboration about 15 years ago in $pn \to \pi^0\pi^0 d$ [45] and $pd \to d\pi^0\pi^0 p$ [46] reactions. It was assigned as the D_{03} state having the $\Delta\Delta$ configuration with mass of 2380 MeV/c^2 and a width of ~70 MeV/c^2. This dibaryon was also observed in reaction of the deuteron photodisintegration [47, 48]

at the beam asymmetry and the neutron polarization measurements.

Now the $d^*(2380)$ is considered as well established, and some its properties such as magnetic moment ($\mu_{d^*} \approx 7.6\mu_N$) were determined [6]. According to [49], the $d^*(2380)$ has three wave function components corresponding to compact bound system of six quarks, and to two $\Delta\Delta$ in the s and d states. Spatial extent of these components are ~0.5, ~0.8, ~1.4 fm respectively, where the bound $|6q\rangle$ term wave function dominates, accounting for ~69% [6]. The compact nature of $d^*(2380)$ differs from the structure of the deuteron, and may have important astrophysical implications, e.g., in describing the internal structure of high-density neutron stars [50].

Second, the ELPH collaboration discovered a possible manifestation of dibaryon states in the reaction $\gamma d \to \pi^0\pi^0 d$ [44]. It was shown that the cross section of this reaction is well described by three isoscalar dibaryons with masses of 2.38, 2.47, and 2.63 GeV/c^2. Moreover, the invariant mass distribution of $\pi^0 d$ in this reaction exhibits a peak with a mass of 2.14 GeV/c^2, which can be identified as a manifestation of the isovector dibaryon D_{12}.

4.2. THE $\gamma d \to \pi^0\pi^0 d$ REACTION

The $\gamma d \to \pi^0\pi^0 d$ reaction cross section and π^0d invariant mass are shown in Figs. 4.3 and 4.4. Analysis [6, 40] has shown the data are well fitted by three Breit–Wigner (BW) functions with isoscalar dibaryon states 2380, 2470, and 2630 MeV/c^2 proposed by the ELPH collaboration [44] (see Fig. 4.3). The lowest of these states has the mass and width of the d*(2380) dibaryon.

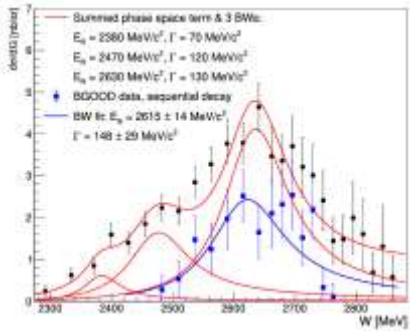


Fig. 4.3. $\gamma d \to \pi^0\pi^0 d$ differential cross section for $\cos\theta_d^{CM} > 0.8$. The error bars are the statistical and systematic uncertainties summed quadratically. A fit including three BW functions are shown as the red lines. The blue squares and line are the differential cross section corresponded to the $\pi^0 d$ invariant mass distributions shown in Fig. 4.4, and BW function fit with the mass and width labelled inset. Figure from Ref. [6]

Neither the traditional coherent model [51] nor the toy pickup model of t-channel $\Delta\Delta$ production shown in Fig. 4.5,a, where final state nucleons coalesce to form a deuteron, describe the experimental data.

The π^0d invariant mass distribution shows a peak at 2114 MeV/c^2 (see Fig. 4.4), which is consistent with the isovector dibaryon observed by the ELPH collaboration, except for the width, which is significantly smaller.

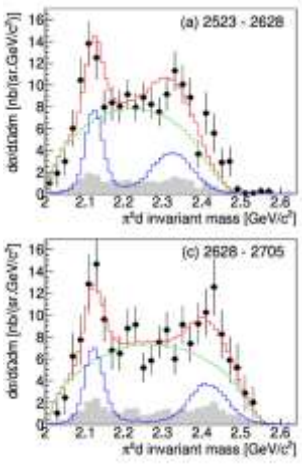


Fig. 4.4. Differential cross section (black points) versus the invariant mass of the $\pi^0 d$ system for $\cos\theta_d^{CM} > 0.8$, W intervals labelled inset, the systematic uncertainties are the grey bars. The fitted distribution to the $\pi^0 d$ invariant mass (red line) is comprised of phase space (green line) and proposed sequential dibaryon decay contributions (blue line). Figures from Ref. [6]

Overall, the distribution is well approximated by simulations incorporating the reaction phase space and a mechanism based on the sequential decay of an isoscalar dibaryon to an isovector one (Fig. 4.5,b). The differential reaction cross section corresponding to the π^0d invariant mass distribution is well described by the BW fit with the proposed 2630 MeV/c^2 dibaryon and confirms the sequential decay mechanism from an isoscalar dibaryon to an isovector one.

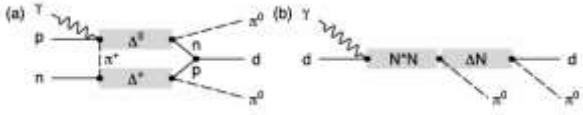


Fig. 4.5. Possible mechanisms contributing to the $\gamma d \to \pi^0\pi^0 d$ reaction: a – The toy pickup model; b – A sequential dibaryon decay mechanism. Figure from Ref. [40]

4.3. $\gamma d \to \pi^0\eta d$ AND $\gamma d \to \pi^0\pi^0\pi^0 d$ REACTIONS

In contrast to the reaction $\gamma d \to \pi^0\pi^0 d$, the shape of differential cross section of the $\gamma d \to \pi^0\eta d$ reaction is well fitted by the toy model (Fig. 4.6), which assumes a quasi-free mechanism, shown in Fig. 4.7 and does not require the involvement of the dibaryons.

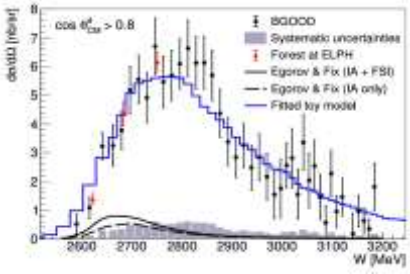


Fig. 4.6. The $\gamma d \to \eta\pi^0 d$ differential cross section [41] for $\cos\theta^d_{CM} > 0.8$ (black circles), data from the ELPH [52] (red triangles). Solid and dashed lines are the phenomenological models [53] with or without the inclusion of final state interactions respectively. Figure from Ref. [6]

According to the model, either the $\Delta(1232)$ or $N(1535)$ resonance is formed with a pion, which then interacts with a spectator nucleon, forming a $N(1535)$ or $\Delta(1232)$ resonance, respectively. After the subsequent decay of the resonances with the emission of a π and η, the nucleons merge into deuteron if there is a small relative momentum between them. The contribution of the diagram Fig. 4.7,a is ten times higher than that shown in Fig. 4.7,b, and it can produce a peak in the cross section around W~2770 MeV, which is the sum of the Δ and N(1535) masses.

Analysis of the $\pi^0\eta$, π^0d and ηd invariant mass distributions [41] has shown that the toy model gives a reasonable description of shape for the $\pi^0\eta$ system in the total range of the measurements, W=2576…3189 MeV, but for π^0d system only in the lower energy interval W=2576…2988 MeV.

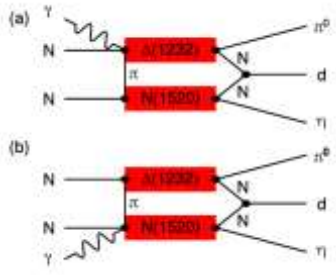


Fig. 4.7. Two proposed mechanisms contributing to the cross section. Figure from Ref. [41]

In the higher interval W= 2899 to 3189 MeV, the data appears to weak peak with a mass of ~2.1 GeV/c^2 which would be consistent with the isovector dibaryon observed in the $\pi^0\pi^0 d$ channel by the ELPH collaboration [44], and disagree with the toy model prediction. The toy model also does not describe the ηd system invariant mass distribution.

Regarding the $\gamma d \to \pi^0\pi^0\pi^0 d$ reaction (see Fig. 4.1) data analysis is currently incomplete. Its energy distribution peaks at ~2.7 GeV, and below this peak the cross section practically coincides with the $\gamma d \to \pi^0\pi^0 d$ reaction which is described by the three aforementioned dibaryons. But, at the energy W≥2.7 GeV, it agrees well with the $\gamma d \to \pi^0\eta d$ cross section, which shape is well described by the toy model in this energy range. As was noted in [6], if such mechanism is dominant, it is possible to explain the similarity of these coherent reactions, $\pi^0\pi^0$d, $\pi^0\eta$d and $\gamma d \to \pi^0\pi^0\pi^0 d$, since N(1535) decays into η, π and $\pi\pi$ with close branching ratios of 30…55, 32…52, and 4…31%, respectively. In this case, the possible contribution of the dibaryons to these reactions mechanisms should be revised. As a whole, these reaction mechanisms remains unclear.

5. FUTURE DEVELOPMENT OF THE UNCONVENTIONAL HADRON STRUCTURE PROGRAM

Hadron spectroscopy researches at ELSA has been ongoing for over 15 years at two facilities, CBELSA/TAPS and BGOOD. During this time, the main objectives of the assigned scientific tasks were achieved, a large amount of data has been collected. Naturally, the time has come to summarize the results and outline new goals for future research, taking into account new technology, up to date experimental technique and data processing. The European expert community highly praised the scientific results obtained at the ELSA facilities and recommended continuing the research, because they believe that hadron spectroscopy is the subject of large-scale experimental research worldwide, which could significantly change the face of nuclear physics in the coming years ([5], p. 19–20).

So, it was decided to continue research in the field of hadron spectroscopy and the search for exotic quark states in the region of light quarks in ELSA facility at the Bonn University, and, in connection with this, to modernize and expand the capabilities of the experimental facility, within the frame of new project called INSIGHT. This project was presented for discussion in some conferences [6–8, 54] and is a part of broader research program in Germany that will be carried out within a special Cluster of Excellence “Color meets Flavor” [9].

5.1. INSIGHT EXPERIMENT AT ELSA

The INSIGHT project assumes to combine the capabilities of the BGOOD and CBELSA/TAPS experiments and create a single facility with improved characteristics, the most important of which are: virtually complete angular coverage for high-resolution detection of photons and charged particles; the ability to perform measurements using linearly and circularly polarized photon beams and polarized proton and deuteron targets. The facility setup is shown in Fig. 5.1.

The new facility will be located on CBELSA/TAPS beam line of the ELSA, and will include: (i) a photon tagging system; (ii) two photon calorimeters for high resolution photon measurements – the main calorimeter (Crystal Barrel, consisting of 1230 CsI(Tl) crystals) used in the CBELSA/TAPS experiment, and a new forward endcap calorimeter (PANDA Forward Endcap) consisting of 3856 $PbWO_4$ crystals; (iii) a new vertex pixel detector located between the target and the main photon calorimeter for detecting charged particles, reconstructing their trajectories and vertices with good resolution; (iv) a new forward spectrometer for detecting charged particles under small angles and determination their momentum. It will consist of a new dipole magnet with high resolution track detectors located above and below magnet, and a system of time-of-flight detectors. The modernization of the facility is planned to be completed within five years, but the launch and beginning of experimental work is planned to take place as the equipment is manufactured and installed, and may begin in two or three years.

The INSIGHT project will continue to investigate the unconventional baryon and dibaryon structures observed in the BGOOD experiment, including the question of whether exotic states exist in the light quark sector, using the opportunities offered by new technologies and the enormous potential of polarization measurements. Some aspects of the proposed research program are discussed in the reports [8, 54], and the methods and implementation pathways are considered with help of the Cluster of Excellence [9].

5.2. THE CLUSTER OF EXCELLENCE "COLOR MEETS FLAVOR"

The Cluster of Excellence "Color meets Flavor" [9] combine research groups from Bonn, Dortmund, Siegen, Jülich and world-renowned experts in strong and weak interaction physics leading experiments and researches in this field. They aim to search for fundamental questions about the nature of matter, the mechanisms formation of matter by the strong "color" forces, the asymmetry between matter and antimatter in the Universe and how is it related to the different "flavors" of quarks seen in the weak interaction, and are there yet unknown particles or forces. Since quarks are not observed as free particles but form bound states, their study requires a precise understanding of both the strong force responsible for their binding and the weak force involved in their decays. As noted in [9], one of the most exciting results in particle physics of recent years are observation of exotic bound states of quarks.

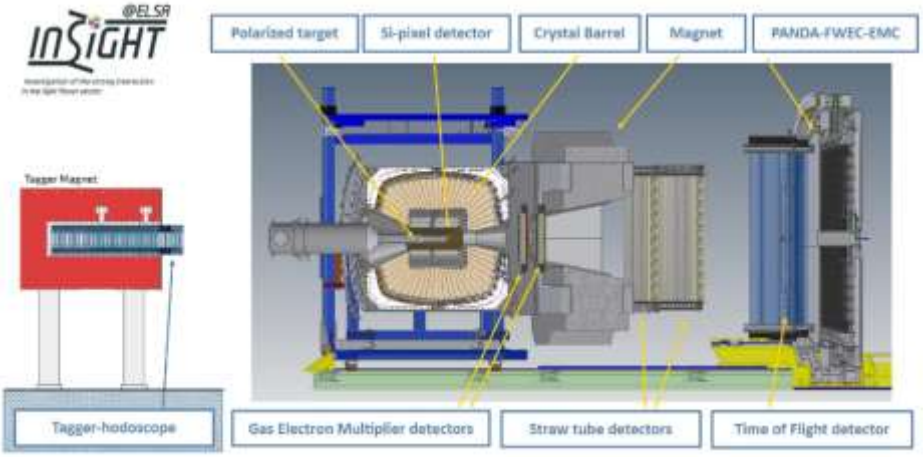


Fig. 5.1. The new INSIGHT experiment at the ELSA facility at the University of Bonn. Figure from Ref. [54]

The Cluster is structured into four Research Areas (RA) and two Technology Areas (TA), the goals of which activity are: bound states of light and heavy quarks (RA1); decays of bottom, charm, and strange quarks (RA2); top quark and Higgs boson (RA3); search for the axion (RA4); instrumentation (TA1) and computational methods (TA2).

The new INSIGHT experiment at ELSA is included in the RA1 and will focus on investigating the spectra of both non-strange and strange baryons, searching for exotic multiquark and molecular states, elucidating the nature of exotic hadrons, and gaining new insights into QCD. Research on hadron structure at RA1 will be conducted in close collaboration with the RA2, which is searching for phenomena in weak decays.

Innovative detector technologies and electronics developed in the TA1 are aimed at supporting future experiments, and firstly, the INSIGHT experiment at ELSA. This includes the development of intelligent experimental hardware that will provide a needed environment for applying breakthrough advances in detector and electronic technologies.

TA2 activities focus on developing new methods and applying advanced computing technologies across all research areas within the Cluster of Excellence, including the development of new quantum computing hardware in computational physics, data analysis, and sophisticated Monte Carlo methods to improve the accuracy of simulations and reconstructions. Some additional information is given in the Appendix B.

CONCLUSIONS

According to NuPECC expert estimates, hadron spectroscopy and the search for exotic hadronic states will be important research area in particle and nuclear physics in the coming decades. The BGOOD collaboration at the ELSA facility has made a significant contribution to this field in the light quark sector. A large body of experimental data has accumulated, complementing the results of research conducted in the heavy quark sector, which indicate the possible existence of the exotic states and dibaryons formed by *uds* quarks.

The new INSIGHT experiment at the ELSA facility aims to continue this research at a higher experimental level. A particular advantage of the facility, opening up unique possibilities, is the availability of a linearly and circularly polarized photon beam and polarized targets, enabling polarization experiments and the acquisition of data for partial waves amplitude analysis.

This research will be supported by a wide range of specialists working in this field, united within the Cluster of Excellence "Color meets Flavor" [9] program. This Cluster has the potential to become a new leading European research center, coordinating and guiding the development of scientific research in nuclear and particle physics in this energy range.

It is particularly noteworthy that the renovated facility and planned research there, supported by the Cluster of Excellence, provide unique opportunities to train students and young professionals in detector operation, experimental measurement methods, and data processing, which are often difficult to achieve in large collaborations. They also provide the necessary knowledge and experience for successful work in both applied physics and in industry.

APPENDIX A

The current BGOOD collaboration: D.D. Burdeinyi[1], A.J. Clara Figueiredo[2], P.L. Cole[3], R. Di Salvo[4], A. Fantini[4,5], O. Freyermuth[2], F. Frommberger[2], V.B. Ganenko[1], J. Groß[2], T.C Jude[2] (spokesperson), K. Kohl[2], P. Levi Sandri[6] (spokesperson), A. de Lope Fend[2], M. Ludwig[2], L. Lutter[2], P. Pedroni[7], M. Romaniuk[8], H. Schmieden[2] (previous spokesperson) and A. Sonnenschein[2].

[1]Kharkiv Institute of Physics and Technology, Kharkiv, Ukraine.

[2]Bonn Universität, Physikalisches Institut, Germany.

[3]Lamar University, Department of Physics, Texas, USA.

[4]INFN Roma, Italy.

[5]Universitá di Roma, Italy.

[6]INFN – Laboratori Nazionali di Frascati, Italy.

[7]INFN sezione di Pavia, Italy.

[8]Institute for Nuclear Research of NASU, Kyiv, Ukraine.

However, as was presented in [55], in reality, from 2008 to 2025, 124 people from 19 institutes in 7 countries took part in the BGOOD collaboration.

The first beam run was performed on January 25, 2010, but the full-scale data acquisition began in April 2017 and continued until December 2025. Total beam time of data taking took 241 days and total cost of these measurements was ~€3.2 million (~€15,000 per day).To date, the following have been produced:

- 9 publications in renowned scientific journals;
- 10 successfully defended PhD theses;
- 25 master theses;
- 27 bachelor theses.

APPENDIX B

The Cluster is structured into four Research Areas, **RA1-RA4,** and two Technology Areas, **TA1, TA2,** the main goals of which activity are [9]:

RA1: Bound states of light and heavy quarks. The new experiment INSIGHT at ELSA is included in RA1 Area and will be aimed to investigate both non-strange and strange baryon spectra, with special efforts directed toward the search for multi-quark and molecular states. Emphasis is placed on clarifying the nature of exotic hadrons and uncovering insights about QCD. This Research Area aims to deepen understanding of the spectrum, properties, and internal structure of hadrons.

RA2: Decays of bottom, charm, and strange quarks. Within RA2, new phenomena in weak decays are being actively searched for in close collaboration with investigations of hadronic structure in RA1. Efforts are directed toward clarifying the origin of flavor anomalies, with both theoretical and experimental approaches being combined to conduct stringent tests of the Standard Model.

RA3: Top quark and Higgs boson. The focus of RA3 lies on the two most massive particles in the Standard Model, the top quark and the Higgs boson. Precision measurements and predictions are being carried out at the highest accessible energies to enhance understanding of fundamental particle interactions. Efforts are underway to identify additional sources of CP violation within top-quark and Higgs decays as potential indicators of new physics. Furthermore, connections between measurements and predictions across all energy scales will be carefully examined to detect effects that may lie beyond the Standard Model.

RA4:Search for the axion. The future babyIAXO experiment will be shaped within RA4. A new cavity-based haloscope experiment will be designed, constructed, and prepared for operation to further the search for dark matter candidates. Additionally, pioneering searches for axions will be conducted at the Belle II, BESIII, and LHCb experiments, expanding the potential to detect these elusive particles. Together, these initiatives aim to advance the search for axions and enhance our understanding of fundamental particles and forces.

TA1:Instrumentation. The Technology Area TA1 will performed a long-standing expertise in instrumentation covering a wide range of detection techniques and associated electronics. Innovative detector technologies and electronics will be developed to support future experiments and push the boundaries of current capabilities, firstly to set up a new, worldwide unique experiment, the INSIGHT experiment at ELSA. Additionally, a dedicated laboratory, the Intelligent Hardware Lab (IHL), will be established to focus on the development of intelligent hardware, providing a specialized environment for pioneering advancements in detector and electronics technologies.

TA2: Computational Methods. TA2 aims at the development of novel techniques and the employment of cutting-edge methods across all Research Areas. In support, the Innovative Algorithms Lab (IAL) will be founded and resources such as the exascale computer JUPITER at Forschungszentrum Jülich and novel quantum computing hardware will be established and exploited. Sophisticated Monte Carlo methods will be implemented to improve simulation accuracy, while new machine learning techniques for computational physics, data analysis, and reconstruction will be introduced in collaboration with leading AI experts. Quantum computing and tensor networks will be pioneered within particle physics to explore their potential in solving complex problems. Additionally, advancements in computer algebra will be pursued in collaboration with experts in mathematics, driving forward the analytical capabilities of particle physics research.

ACKNOWLEDGEMENTS

I am deeply grateful to Tom Jude for his support, valuable advices and comments.

REFERENCES

1. (BGOOD Collaboration), S. Alef, et al. // *Eur. Phys. J. A.* 2020, v. 56, p. 104; http://dx.doi.org/10.1140/epja/s10050-020-00107-x

2. E. Aker et al. // *Nucl. Instrum. Meth. A.* 1992, v. 321, p. 69; http://dx.doi.org/10.1016/0168-9002(92)90379-I

3. A.R. Gabler et al. // *Nucl. Instrum. Meth. A.* 1994, v. 346, p. 168; http://dx.doi.org/10.1016/0168-9002(94)90701-3

4. NuPECC Long Range Plan 2017 for European Nuclear Physics.

5. NuPECC Long Range Plan 2024 for European Nuclear Physics.

6. T.C. Jude. Studies of unconventional baryon structure in the light quark sector with the BGOOD photoproduction experiment // *Progress in Particle and Nuclear Physics.* 2026, v. 147, p. 104224.

7. (BGOOD Collaboration), T.C. Jude, et al. Studies of unconventional baryon structure in the light quark sector with the BGOOD photoproduction experiment // *Proceedings of Science Hadron 25 conference*, 2025.

8. U. Thoma. Light baryon spectroscopy (@ELSA), Bonn. International School of Nuclear Physics. 44th Course: From quarks and gluons to hadrons and nuclei, Erice-Sicily, September 18-24, 2023. Blackett Institute (San Domenico).

9. https://color-meets-flavor.de.

10. *Standard Model of Elementary Particles*, url: https://en.wikipedia.org/wiki/Standard_Model

11. S. Alef. *Studies of $\eta'p$ photoproduction at the BGOOD experiment*: PhD thesis. Rheinischen Friedrich-Wilhelms-Universitat Bonn, 2021.

12. G. Scheluchin. *$\Lambda(1405)$ photoproduction with the BGO-OD experiment*: PhD thesis. The University of Bonn, 2019.

13. F.-K. Guo, C. Hanhart, U. G. Meißner, Q. Wang, Q. Zhao, B.-S. Zou. Hadronic molecules // *Rev. Modern Phys*. 2018, v. 90; http://dx.doi.org/10.1103/RevModPhys.90.015004, (2018), 015004

14. (LHCb Collaboration), R. Aaij, et al. Observation of a Narrow Pentaquark State, $P_c(4312)^+$, and of the Two-Peak Structure of the $P_c(4450)^+$ // *Phys. Rev. Lett*. 2019, v. 122, p. 222001; http://dx.doi.org/10.1103/PhysRevLett.122.222001

15. H. Huang, X. Zhu, J. Ping. Pc-like pentaquarks in a hidden strange sector // *Phys. Rev*. *D*. 2018, v. 97, p. 094019; http://dx.doi.org/10.1103/PhysRevD.97.094019

16. (CLAS Collaboration), B.A. Mecking, et al. // *Nucl. Instrum. Meth*. *A*. 2003, v. 503, p. 513; http://dx.doi.org/10.1016/S0168-9002(03)01001-5

17. (A2 Collaboration), S. Schumann, et al. // *Eur. Phys. J. A.* 2010, v. 43, p. 269; http://dx.doi.org/10.1140/epja/i2010-10925-y

18. T. Nakano et al. // *Nucl. Phys. A*. 2001, v. 684, p. 71; http://dx.doi.org/10.1016/S0375-9474(01)00490-0

19. (GRAAL Collaboration), Bartalini, et al. // *Eur. Phys. J. A*. 2005, v. 26, p. 399; http://dx.doi.org/10.1140/epja/i2005-10191-2

20. J. Allison et al. // *Nucl. Instrum. Meth*. *A*. 2016, v. 835, p. 186; http://dx.doi.org/10.1016/j.nima.2016.06.125

21. M.-L. Du, V. Baru, F.-K. Guo, C. Hanhart, U.-G. Meißner, J.A. Oller, Q. Wang // *Phys. Rev. Lett*. 2020, v. 124, p. 072001; http://dx.doi.org/10.1103/PhysRevLett. 124.072001

22. (BGOOD Collaboration), T.C. Jude, et al. *// The study of unconventional baryon structure via strangeness photoproduction at the BGOOD experiment:* NSTAR2024, York 19th July 2024.

23. (BGOOD Collaboration), T.C. Jude, et al. // *Phys. Lett. B*. 2021, v. 820, p. 136559; http://dx.doi.org/10.1016/j.physletb.2021.136559

24. J. Groß. Ph.D. thesis. The University of Bonn, 2025.

25. (CBELSA/TAPS Collaboration), R. Ewald, et al. // *Phys. Lett. B*. 2012, v. 713, p. 180; http://dx.doi.org/10.1016/j.physletb.2012.05.066

26. (BGOOD Collaboration), K. Kohl, T.C. Jude, et al. // *Eur. Phys. J. A*. 2023, v. 59, p. 254; http://dx.doi.org/10.1140/epja/s10050-023-01133-1

27. (BGOOD Collaboration), G. Scheluchin, T.C. Jude, et al. // *Phys. Lett. B*. 2022, v. 833, p. 137375; http://dx.doi.org/10.1016/j.physletb.2022.137375

28. (CLAS Collaboration), R. Bradford, et al. // *Phys. Rev. C*. 2006, v. 81, p. 035202; http://dx.doi.org/10.1103/PhysRevC.73.035202

29. (CLAS Collaboration), B. Dey et al. // *Phys. Rev. C.* 2010, v. 82, p. 025202; http://dx.doi.org/10.1103/PhysRevC.82.025202

30. (SAPHIR Collaboration), K. Glander, et al. // *Eur. Phys. J. A*. 2004, v. 19, p. 251; http://dx.doi.org/10.1140/epja/i2003-10119-x

31. (LEPS Collaboration), M. Sumihama, et al. // *Phys. Rev. C.* 2006, v. 73, p. 035214; http://dx.doi.org/10.1103/PhysRevC.73.035214

32. (LEPS Collaboration), S.H. Shiu, H. Kohri, et al. // *Phys. Rev. C*. 2018, v. 97, p. 015208; http://dx.doi.org/10.1103/PhysRevC.97.015208

33. A.V. Anisovich et al. // *Eur. Phys. J. A*. 2014, v. 50, p. 129; http://dx.doi.org/10.1140/epja/i2014-14129-3

34. (LEPS Collaboration), H. Kohri, et al. // *Phys. Rev. Lett*. 2006, v. 97, p. 082003; http://dx.doi.org/10.1103/PhysRevLett.97.082003

35. (CLAS Collaboration), S.A. Pereira, et al. // *Phys. Lett. B*. 2010, v. 688, p. 289; http://dx.doi.org/10.1016/j.physletb.2010.04.028

36. N.-C. Wei, A.-C. Wang, F. Huang. // *Phys. Rev. D*. 2023, v. 107, p. 14018; http://dx.doi.org/10.1103/PhysRevD.107.114018

37. A. Ramos, E. Oset // *Phys. Lett. B*. 2013, v. 727, p. 287; http://dx.doi.org/10.1016/j.physletb.2013.10.012

38. A. Martínez Torres, K.P. Khemchandani, U.G. Meißner, E. Oset // *Eur. Phys. J. A*. 2009, v. 41, p. 361; http://dx.doi.org/10.1140/epja/i2009-10834-2

39. (A2 Collaboration), C.S. Akondi, K. Bantawa, et al. // *Eur. Phys. J. A*. 2019, v. 55, p. 202; http://dx.doi.org/10.1140/epja/i2019-12924-x

40. (BGOOD Collaboration), T.C. Jude, et al. // *Phys. Lett. B*. 2022, v. 832, p. 137277; http://dx.doi.org/10.1016/j.physletb.2022.137277

41. A.J.C. Figueiredo, T.C. Jude, et al. // *Coherent $\pi^0\eta$ photoproduction at forward deuteron angles measured at BGOOD*, 2024; http://dx.doi.org/10.48550/arXiv.2405.09392, arXiv:2405.09392

42. R. Volk. *Investigation of the Coherent $\gamma D \to \pi^0\pi^0\pi^0 D$ Reaction at the BGOOD Experiment* (*Master's thesis*). The University of Bonn, 2024.

43. F.J. Dyson, N.-H. Xuong // *Phys. Rev. Lett*. 1964, v. 13 (26), p. 815; http://dx.doi.org/10.1103/PhysRevLett.13.815

44. (FOREST at ELPH Collaboration), T. Ishikawa, et al. // *Phys. Lett. B.* 2019, v. 789, p. 413.
45. (CELSIUS/WASA Collaboration), M. Bashkanov, et al. // *Phys. Rev. Lett*. 2009, v. 102, p. 052301; http://dx.doi.org/10.1103/PhysRevLett.102.052301
46. (WASA-at-COSY Collaboration), P. Adlarson, et al. // *Phys. Rev. Lett*. 2011, v. 106, p. 242302; http://dx.doi.org/10.1103/PhysRevLett.106.242302
47. (A2 Collaboration), M. Bashkanov, et al. // *Phys. Lett. B.* 2019, v. 789, p. 7; http://dx.doi.org/10.1016/j.physletb.2018.12.026, 2019
48. M. Bashkanov, D.P. Watts, *J. Phys. G. Nucl. Part. Phys.* 2020, v. 47, p. 03LT01; http://dx.doi.org/10.1088/1361-6471/ab67e8 2020
49. F. Huang, Z.Y. Zhang, P.N. Shen, W.L. Wang // *Chinese J. Phys*. 2015, v. 7, p. 071001; http://dx.doi.org/10.48550/arXiv.1408.0458
50. I. Vidaña, M. Bashkanov, D.P. Watts, A. Pastore // *Phys. Lett. B.* 2018, v. 781, p. 112; http://dx.doi.org/10.1016/j.physletb.2018.03.052
51. A. Fix, H. Arenhövel // *Eur. Phys. J. A.* 2005, v. 25, p. 115; http://dx.doi.org/10.1140/epja/i2005-10067-5
52. (FOREST at ELPH Collaboration), T. Ishikawa, et al. // *Phys. Rev. C.* 2022, v. 105, p. 045201; http://dx.doi.org/10.1103/PhysRevC.105.045201
53. M. Egorov, A. Fix // *Phys. Rev. C.* 2013, v. 88, p. 054611; http://dx.doi.org/10.1103/PhysRevC.88.054611
54. U. Thoma. *Physics with the new INSIGHT experiment @ELSA*: Collaboration Meeting, Jun 18-19, 2026, Bonn, Germany; https://indico.hiskp.uni-bonn.de/event/1624/
55. K. Kohl. *BGOOD over the years*: BGOOD Collaboration Meeting, Jun 18-19, 2026, Bonn, Germany; https://indico.hiskp.uni-bonn.de/event/1624/

Article received 18.07.2026

КОЛАБОРАЦІЯ BGOOD ТА ПОШУК НЕТРАДИЦІЙНИХ БАРІОННИХ СТАНІВ У СЕКТОРІ ЛЕГКИХ *uds*-КВАРКІВ

В.Б. Ганенко від імені BGOOD колаборації

Представлено огляд експериментів BGOOD на електронному прискорювачі ELSA (Боннський університет, Німеччина), присвячених дослідженню фотонародження баріонів із дивністю та без (strange and non-strange baryon). Експеримент BGOOD спеціально розроблений для вимірювання цих процесів за низької передачі імпульсу до залишкової адронної системи, тому він особливо підходить для пошуку екзотичних молекулярно-подібних баріонних станів у секторі легких кварків (*uds*), які можуть бути еквівалентними пентакварковим P_C-станам, які спостерігалися в секторі *c*-кварків. Результати когерентного фотоутворення $\pi^0\pi^0$-, $\pi^0\eta$- та $\pi^0\pi^0\pi^0$-мезонів на дейтроні демонструють великі диференціальні перерізи для цих реакцій, механізм яких ще незрозумілий. Це може бути пов'язано як із дибаріонами, так і з якимись процесами перерозсіювання.